8. Picard R.W. Affective computing. – Cambridge, MA: MIT Press, 1997. – 292 p.
9. Mollahosseini A. AffectNet: a database for facial expression, valence, and arousal computing in the wild / A. Mollahosseini, B. Hasani, M.H. Mahoor // IEEE Transactions on Affective Computing. – 2019. – Vol. 10, No. 1. – P. 18–31.

UDC 621.396.67

A WIDEBAND PRINTED MONOPOLE ANTENNA WITH CIRCULAR POLARIZATION

V.L. Pham, PhD student at Dept. of television and control
Scientific supervisor V.P. Kosteletskii, associate professor at Dept. of Quantum Radio Engineering, TUSUR, PhD in Engineering Science
Tomsk, TUSUR, pham.v.2213-2025@e.tusur.ru

This paper presents a wideband printed monopole antenna with circular polarization (CP), achieved by employing an asymmetric radiating element. The proposed antenna operates effectively over the frequency range of 3.26–7.46 GHz with a return loss below −10 dB, an axial ratio (AR) of less than 3 dB obtained within the 4.4–7.3 GHz band and an average maximum gain of 3.7 dBi.
Keywords: wideband antenna, circular polarization, patch antenna, asymmetric radiating element, gain.

Modern wireless telecommunication systems are characterized by increasingly stringent requirements for antenna performance. Therefore, the development of a wideband antenna with circular polarization (CP) is important [1]. Additionally, printed monopole antennas are popular because of their ease of fabrication and ability to provide broad impedance bandwidth; however, they typically exhibit linear polarization [2]. This work investigates a printed monopole antenna that combines simple design, extended suitable bandwidth, and CP capability.

Methods. The substrate of the proposed antenna is Taconic RF-30 material with a dielectric constant of 3 and a loss tangent of 0.0019. The antenna configuration and design steps are illustrated in Fig. 1 and 2. In [3], it is shown that that shifting the feed line from the center of the substrate brings the input impedance close to 50 Ω and broadens the impedance bandwidth. In this design, the feed line is offset by 5.5 mm from the center of the structure, as shown in Fig. 2, *b*. To improve the axial ratio (AR), the upper-right and lower-left corners of the radiating element are truncated, as shown in Fig. 2, *c* [4]. In addition, a rectangular slot is etched in the ground plane beneath the feed line on the back side of the substrate, as shown in Fig. 2, *d*, which improves the impedance bandwidth [5] and broadens the bandwidth over which CP is maintained. All design stages were carried out using CST Studio Suite. The antenna parameters are presented in the table below.

Antenna parameters and their values

Parameter	*W*	*L*	*c*	*dx*	*a*	*b*	*g*	*h*
Meaning (mm)	40	16	2	5.5	4	2	11.75	1.52

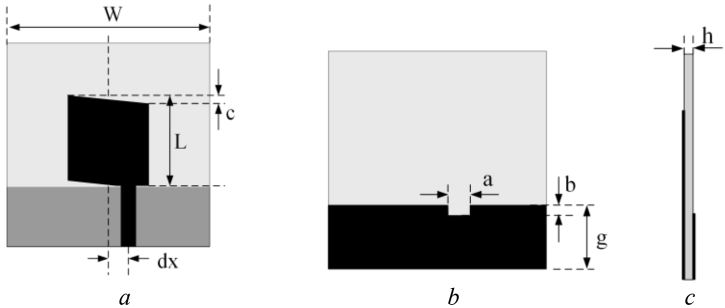

Fig. 1. Proposed antenna configuration:
top view (*a*), bottom view (*b*) and side view (*c*)

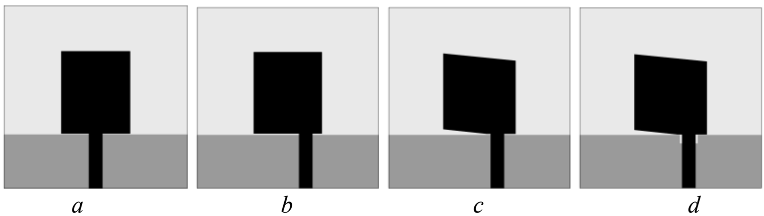

Fig. 2. Design steps of the proposed antenna:
step 1 (*a*), step 2 (*b*), step 3 (*c*) and step 4 (*d*)

Results and Discussion. The simulated return loss is shown in Fig. 3. The simple antenna in the first step achieved a relatively wide impedance bandwidth of 2.8–4.8 GHz. By offsetting the feed line, the bandwidth is further extended to 2.9–6.5 GHz in step 3. Finally, the optimized antenna in step 4 achieved an impedance bandwidth from 3.26 to 7.46 GHz.

A comparison of AR at each design step and the peak gain of the proposed antenna over the operating frequency band are presented in Fig. 4. The simulation results show that offsetting the feed line from the center of the radiating patch enables CP. Further modification of the antenna in steps 3 and 4 results in an AR below 3 dB from 4.4 to 7.3 GHz. The maximum-gain curve over the operating band indicates that the proposed antenna achieves an average value of approximately 3.7 dBi.

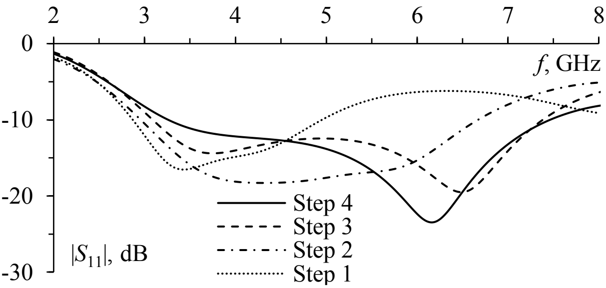

Fig. 3. Simulated return loss at each design step

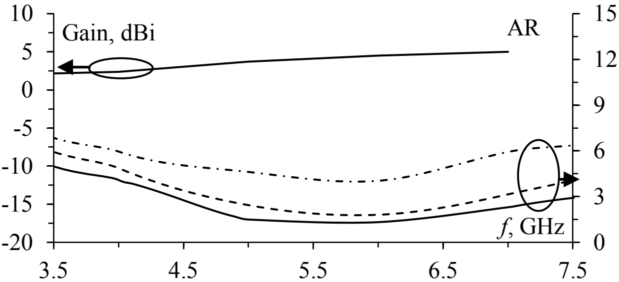

(–·–·–) – step 2, (-----) – step 3, (——) – step 4

Fig. 4. Simulated AR at each design step and maximum gain of proposed antenna

Conclusion. This paper presents a wideband printed monopole antenna with CP, achieved by offsetting the feed line from the center, modifying the shape of the radiating element, and introducing slots in the ground plane. The proposed printed monopole antenna is suitable for various wireless communication systems, such as unmanned aerial vehicles and wireless sensor networks. The research was funded by the Ministry of Science and Higher Education of the Russian Federation, project FEWM-2026-0007.

REFERENCES

1. Banerjee U. A review on circularly polarized antennas, trends and advances / U. Banerjee, A. Karmakar, A. Saha // International Journal of Microwave and Wireless Technologies. – 2020. – Vol. 12, No. 9. – P. 1–22.

2. Broadband monopole antenna with wide-band circular polarization / B. Chen, Y.-C. Jiao, F.-C. Ren, L. Zhang // Progress in Electromagnetics Research Letters. – 2012. – Vol. 32. – P. 19–28.

3. An effective technique based on off-set fed patch to enhance the bandwidth of microstrip planar antenna / R. Azim, R.W. Aldhaheri, M.M. Sheikh, M.T. Islam // Microwave and Optical Technology Letters. – 2016. – Vol. 58, No. 2. – P. 1–6.

4. Keshwala U. Circularly polarized truncated corner square slot antenna for Ku-band applications / U. Keshwala, S. Rawat, K. Ray. // Scientia Iranica. – 2023. – Vol. 30, No. 1. – P. 218–227.
5. Rajappa H.S. Partial ground-based miniaturized ultra wideband microstrip patch antenna / H.S. Rajappa, D.N. Chandrappa, Rajendra Soloni // Indian Journal of Science and Technology. – 2024. – Vol. 17, No. 2. – P. 105–111.

UDC 691.714.018.8

DEVELOPING A COMPOSITE BASED ON STAINLESS STEEL WITH THE ADDITION OF MOLYBDENUM BORIDES BY SPARK PLASMA SINTERING

A. Javaid, MSc Student at Dept. of Material Science;
M.J. Derwesh, MSc Student at Dept. of Material Science;
Y.Z. Vassilyeva, Associate Professor at Dept. of Material Science, PhD in Engineering Science
Tomsk, National Research Tomsk Polytechnic University, da0002@tpu.ru

Conventional austenitic stainless steels lack thermal conductivity and oxidation resistance above 600 °C. However, ultra-high-temperature ceramics are brittle. This work presents a spark plasma sintered 12X18H10T steel reinforced with molybdenum boride which is a multifunctional composite for passive thermal management in harsh-environment power electronics and sensor housings.
Keywords: 12X18H10T stainless steel, molybdenum boride, metal matrix composite, powder metallurgy.

Stainless steel (SS) is the primary candidate whenever developing a mechanical component with superior material properties is required. A widely used austenitic SS is 12X18H10T (or AISI 321) consisting of Fe (70%), Cr (17~19%), Ni (9~11%), Mn (< 2%), Si (< 0.8%), Ti (0.8%) and carbon (< 0.12%) etc., which is known for its corrosion resistance and high strength [1]. In some severe chemical applications, austenitic steel 12X18H10T is not performing efficiently due to lack of properties and electrolyte plasma surface treatment required to enhance hardness [2]. To improve the characterization of SS, world's leading research and development organizations are working on it as a major research frontier. Several studies to improve properties of SS have been conducted. In a study by Sulima et al. [3], 10% zirconium diboride (ZrB_2) and 10% titanium diboride (TiB_2) added in 316L steel by spark plasma sintering (SPS) increased the hardness from 188 HV to 456 HV and 358HV, respectively.

In our study, Russian grade SS 12X18H10T and molybdenum borides (Mo_xB_y) are selected for the integration of metal matrix composite. Mo_xB_y